Journal of Theory, Mathematics and Physics
Vol. 3, No. 11, 2024 ISSN: 2181-4376
Innova Science

THE ROLE OF GRAVITY IN NEUTRINO EMISSION AND HEAVY ELEMENT SYNTHESIS

Annotation:

Astronomical observations offer data on the prevalence of heavy elements, while nuclear physics elucidates the specifics of the reactions occurring between nuclei and the resulting final abundances. The objective is to replicate a specific stellar location's thermodynamic conditions, develop a reaction network under those circumstances, and ultimately reproduce the detected abundances [1]. Nevertheless, there remains debate about the astronomical locations at this stage, and the nuclear characteristics of many of the nuclei involved in the reactions are uncertain.

Information about the authors

Laylo Habibullaeva
Faculty of Physics, Namangan State University, Bobursho Str. 161, Namangan 160107, Uzbekistan

I. INTRODUCTION

Astronomical observations offer data on the prevalence of heavy elements, while nuclear physics elucidates the specifics of the reactions occurring between nuclei and the resulting final abundances. The objective is to replicate a specific stellar location's thermodynamic conditions, develop a reaction network under those circumstances, and ultimately reproduce the detected abundances [1]. Nevertheless, there remains debate about the astronomical locations at this stage, and the nuclear characteristics of many of the nuclei involved in the reactions are uncertain.

Of all these different elements, neutrinos play a key role. Weak interactions can make a medium rich in protons or neutrons [3, 4]. This, along with the thermodynamical progression of the matter, determines the types of elements produced [5, 6].

Different types of physics can impact neutrino flux from stellar sources such as supernovae and black hole accretion disks (both suggested locations for r-process nucleosynthesis), including flavor oscillations and coherent scattering. In prior research, we have explored how gravity affects neutrino emission and the creation of heavy elements in outflows originating from black hole accretion disks [8, 9]. Despite focusing our studies on these particular areas, the effects of strong gravitational fields on neutrino emission are significant in any other environment where neutrinos are copiously generated near massive central objects. Paying attention to the 3D geometry of the source is essential, as relativistic effects depend on the curvature of space-time. We will now examine more details about the influence of general relativity on neutrino fluxes and the formation of heavy elements in black hole accretion disks.

II. INFLUENCE OF GENERAL RELATIVITY ON NEUTRINO EMISSIONS

The powerful gravitational field of a compact object reshapes the space-time geometry in its vicinity. This impacts the neutrino flow detected at a distance from the central object. The principal

consequences of the gravitational field on the fluxes involve energy displacements and the modification of the solid angle that the source appears to occupy from the perspective of the observer $d\Omega_{ob}$ This can be determined by tracking the bending of neutrino paths, which involves locating their null geodesics in a specific curvature. The energy emitted E_{em} and the observed energy E_{ob} are connected by the relation $E_{em} = (1 + z)E_{ob}$ represents the redshift. The observed neutrino flux at a certain distance from the compact object is effective r_{ob}

$$\phi^{eff} = \frac{1}{4\pi} \int d\Omega_{ob} \times \phi_{ob}(E_{ob}). \quad (1)$$

The initial step in converting fluxes from a flat geometry to a curved one is preserving number density in phase space [10]. This results in expressing the detected general relativistic flows as

$$\phi^{eff} \infty \frac{1}{4\pi} \int d\Omega_{ob} \times \frac{E_{ob}^2}{\exp(\frac{Eob(1+z)}{Tem} + 1)} \quad (2)$$

Where has the neutrino Fermi-Dirac distribution been expressed in relation to the temperature at the emission point T_{em} (typically the known value from numerical simulations).Both the redshift $1 + z$ and the solid angle $d\omega_{ob}$ are influenced by the space-time structure and, consequently, by the specifics of the matter distribution of the compact object.

III. THE RATES OF REACTION

A critical factor in determining the type of nuclear products synthesized in an astrophysical site is the proton-to- neutron ratio, or electron fraction Y_e.

If Y_e 0, 5 the medium is proton-rich, while if Y_e 0, 5 , it is neutron-rich. In such settings, the initial thermody- namic state of the substance adjacent to the compact entity causes it to separate into electrons, protons, and neutrons [11]. Next, the primary reactions determining the composition of the matter are:

$$e^+ + n \leftrightarrow p + \nu_e^-, \quad (3)$$

$$e^- + n \leftrightarrow p + \nu_e \quad (4)$$

When the flow of electron neutrinos surpasses that of electron antineutrinos, the inverse reaction outlined in equation 4 will result in the material becoming enriched with protons. In contrast, when the electron antineutrino flux outweighs that of electron neutrinos, the material will become enriched with neutrons. When both neutrino and antineutrino fluxes are feeble, the relevance of forward reactions like electron capture on protons and positron capture on neutrons will exceed that of neutrinos in determining the electron fraction.

The electron fraction Y_e calculated solely based on the reverse reactions of equations 3 and 4 is influenced by the absorption rates of these processes [12]. Since the reaction rates are determined by the neutrino fluxes, which are impacted by a strong gravitational field, Y_e is also influenced accordingly. In relation to the observed fluxes phi^{eff} , the rate of absorption of neutrinos on neutrons can be determined

$$\lambda_{\nu_e n} = b \int_0^{inf} \phi_{\nu_e}^{eff} (E_{ob} + \triangle)^2 \sqrt{1 - \frac{m_e^2}{(E_{ob} + \triangle)^2}} W_m dE_{ob}, \quad (5)$$

and of antineutrinos on protons

$$\lambda_{\nu_e^- n} = b \int_{\triangle + m_e}^{inf} \phi_{\nu_e}^{eff}(E_{ob} - \triangle)^2 \sqrt{1 - \frac{m_e^2}{(E_{ob} - \triangle)^2}} w_m dE_{ob}, \qquad (6)$$

where $W_M = 1 + 1.1\ mn$ and $W_M - = 1\ \_7.1\ mn$ represent the feeble magnetism adjustments, m_n and m_e denote the masses of the neutron and electron respectively,the distinction between neutron and proton masses is indicated,

and $b = 9.70410^{-50} cm^2 keV^2$.

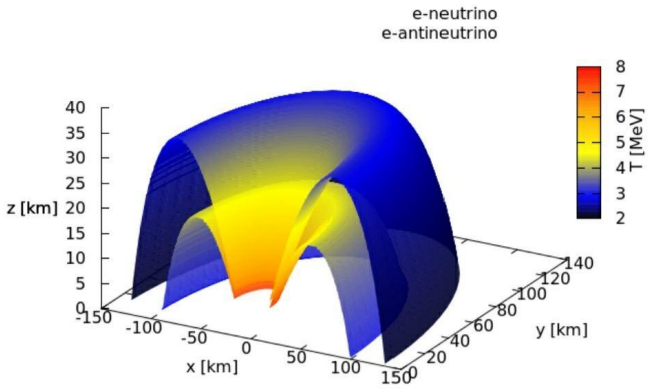

Figure 1. Electron neutrino (outter) and antineutrino (inner) surfaces corresponding to a snapshop at t=20 ms, of a hydrodynamical simulation of a torus around a 3 solar mass black hole.

IV. ASTROPHYSICAL SETTING: EJECTIONS FROM ACCRETION DISKS

A potential situation following the merger of two dense entities (black hole-neutron star or neutron star-neutron star) is the creation of an accretion disk or torus surrounding a black hole. Considering the initial conditions of the progenitors, the material in the disk is rich in neutrons and sufficiently hot to be broken down into nucleons. A portion of this material may be expelled in hot ejections, creating an intriguing situation for the formation of neutron-rich elements.The findings outlined here are derived from a time-dependent hydrodynamic simulation of matter accreting around a 3 solar mass black hole with a spin of a = 0.8.In this situation, neutrinos are abundantly released.The emission points correspond to the neutrino surfaces, the locations where, after being confined by the high-density conditions, neutrinos can move freely.Figure 1 illustrates a transverse section of the electron neutrino and antineutrino surfaces for this disk model at t = 20 ms.The z-axis represents the actual decoupling height, and the color scale indicates the neutrino temperature Tem, which is essential for calculating the neutrino fluxes as outlined in equation 2.The reactions and specifics employed to compute these surfaces are covered. The di erence in the neutrino decoupling surfaces for each flavor, in energy and in distance from the black hole, has important consequences in terms of the effects of gravity on nucleosyntesis.

Journal of Theory, Mathematics and Physics
Vol. 3, No. 11, 2024 ISSN: 2181-4376
Innova Science

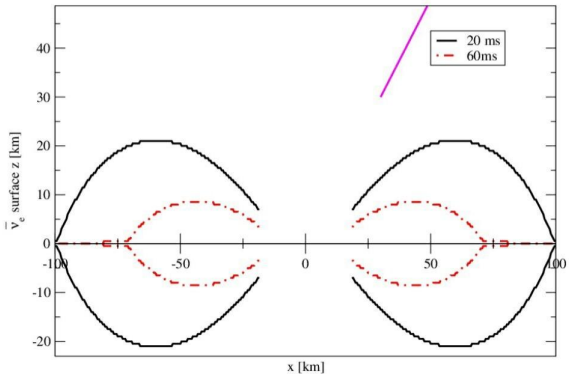

Figure 2. A transversal cut of the electron antineutrino surfaces at two different times, t=20 and 60 ms. The magenta line shows the outflow trajectory starting at x=30 km, z=30 km, It is from this point that we launch the outflow and follow the evolution of the neutrino reaction rates.

For the outflow, we utilize standard neutrino-driven wind paths characterized by entropy and acceleration timescale parameters.Our outflow follows a radial trajectory that begins at r = 30 km from the black hole and stretches out to thousands of kilometers away [13].Figure 2 displays the electron antineutrino surfaces at two different times, t = 20 ms and 60 ms, along with a segment of the outflow trajectory (magenta line).As time progresses and matter is pulled into the black hole, the neutrino surfaces contract.

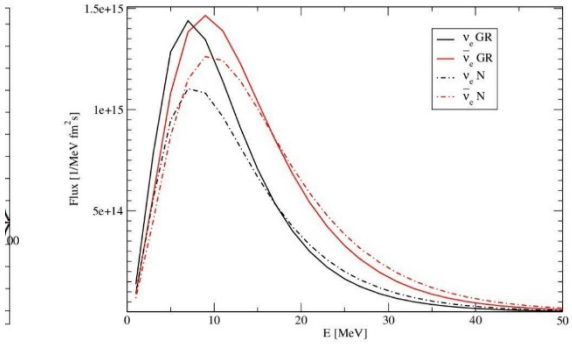

Figure 3. Electron neutrino (black) and antineutrino (red) fluxes as registered at 20 ms at a point located at x=z=100 km from the center of the black hole. The solid lines correspond to a general relativistic calculation of the fluxes while the dotted-dashed lines describe fluxes in a Newtownian calculation.

In this astrophysical context, we evaluate the neutrino fluxes as indicated in equation 2.The reactions in eqs. 3 and 4 occur at specific points in the outflow trajectory, referred to as the observers.Emitters are the locations found on the neutrino surfaces.We find the null geodesics linking each point in the outflow with corresponding points on the neutrino surface.This technique establishes the solid angles $d\Omega_b$. Both the position of the outflow trajectory r_{ob} and the emission points on the neutrino surface r_{em} affect the redshift $1 + z$ Electron antineutrinos are hotter at $t = 20ms$ (as shown by the colored scale in Figure 1) and their fluxes exceed those of electron neutrinos.Regardless of space-time curvature, this is clearly shown by the flux comparison by flavor in Figure 3 (black and red lines), where the fluxes at $z = x = 100km$ are plotted. When factoring in general relativistic effects, the energetic antineutrinos emitted close to the black hole undergo more redshift than the neutrinos.This effect causes a decrease in the large energy tails of the fluxes (compare the dotted-dashed lines representing Newtonian (N) neutrinos with the solid lines for relativistic ones (GR) in Figure 3).Consequently, in curved space-

time, the capture rates of electron antineutrinos are more significantly reduced compared to Newtonian rates, leading to the material becoming less neutron-rich.In

the case of an outflow trajectory with an entropy per baryon of 30, the Newtonian electron fraction Ye^- tends toward

0.47 near $z = x = 100km$, in contrast to the relativistic value of $Ye^- \approx 0.49$. It should be noted, however, that the

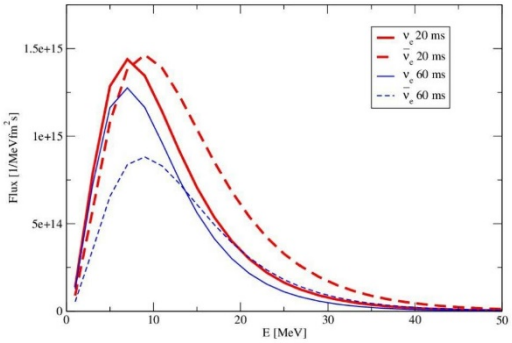

Figure 4. Comparison of electron neutrino (solid) and antineutrino (dashed) fluxes registered at x=z=100 km. Red lines correspond to fluxes at t=20 ms and blue lines to t=60 ms.

emission points are changed by the dynamical evolution, as shown in Figure 2.As shown in Figure 4, the neutrino fluxes at two different times— $t = 20ms$ (red lines) and $t = 60ms$ (blue lines)—are observed from a location at $x_{ob} = z_{ob} = 100km$ from the black hole. At $t = 20ms$, the flux of electron antineutrinos is larger than that of electron neutrinos, as previously discussed (compare solid and dashed red lines).However, at $t = 60ms$ (indicated by the blue lines in Figure 4), the situation reverses, and the electron neutrino fluxes are more prominent.his happens because, as time goes on, more material is drawn into the black hole, and despite both surfaces shrinking, the reduction in the electron antineutrino surface is much more pronounced.Therefore, at $t = 60ms$, neutrino captures on neutrons (as outlined in eq. 4) are predominant, resulting in material that is rich in protons.In the context of general relativity, the decrease in antineutrino fluxes is greater since antineutrinos experience a higher degree of redshift compared to neutrinos [9].As a result, the medium becomes even more proton-rich. In the previously mentioned example, this results in a Newtonian $Ye^- \approx 0.53$, while with general relativity, $Ye^- \approx 0.56$.

V. CONCLUSION

The neutrino flux detected from a source with a massive central body is markedly different from the flux emitted by the same source in a gravitational field in free space.This discrepancy influences the neutrino absorption rates on nucleons, thereby affecting the electron fraction of the medium.The modifications to the electron fraction caused by the gravitational field are significant enough to change the final abundances in nucleosynthesis.Because of the initially low electron fraction of their progenitors, merger-type accretion disks are viewed as promising candidates for the synthesis of heavy, neutron-rich nuclei.We examine the formation of elements that arise in outflows from black hole accretion disks.Our disk model is founded on a hydrodynamical simulation, and the outflow model resembles typical supernova neutrino winds.We discover that gravity significantly influences the electron fraction through its impact on neutrino behavior.The overall variation in the neutrino fluxes is a decrease in the high-energy tails caused by redshifts.This effect is more pronounced in the electron antineutrino channel, resulting in proton-rich material. We find that time evolution is significant, as the neutrino surfaces contract when matter is pulled into the black hole. This reduction in neutrino surfaces, along with the intensified redshifts, results in even greater proton richness in the material.

VI. REFERENCES

1. R. Surman and C. McLaughlin, *Astrophys. J.* **618**, 397 (2004).
2. H. Gutbrod, *FAIR Baseline Technical Report* (2006).
3. Y. Yano, *Nucl. Instrum. Methods Phys. Res. B* **261**, no. 1/2, 1009–1013 (2007).
4. A. Malkus, J. P. Kneller, G. C. McLaughlin, and R. Surman, *Phys. Rev. D* **86**, 085015 (2012).
5. E. Pllumbi, I. Tamborra, S. Wanajo, H.-Th. Janka, L. Huedepoh, arXiv:1406.2596.
6. C. Horowitz, et al., *Phys. Rev. C* **69**, 045804 (2004).
7. H. Sonoda, et al., *Phys. Rev. C* **75**, 042801 (2007).
8. R. Surman, O. L. Caballero, G. C. McLaughlin, O. Just, H.-Th. Janka, *J. Phys. G: Nucl. Part. Phys.* **41**, 044006 (2014).
9. O. L. Caballero, G. C. McLaughlin, and R. Surman, *ApJ* **745**, 170 (2012). [10] C. J. Horowitz, *Phys. Rev. D* **65**, 043001 (2002).
10. O. Just, et al., submitted to *MNRAS* (2014), arXiv:1406.2687.
11. A. B. Balantekin, et al., *Mod. Phys. Lett. A* **29**, no. 11, 1430010 (2014). [13] Y. Z. Qian, et al., *Astrophys. J.* **471**, 331–351 (1996).